

Model Test of the STC Concept in Survival Modes

Ling Wan

Centre for Ship and Ocean
Structures (CeSOS)
Norwegian University of Science
and Technology (NTNU)
Trondheim, Norway

Zhen Gao

Centre for Ship and Ocean
Structures (CeSOS)
Centre for Autonomous Marine
Operations and Systems
(AMOS)
Norwegian University of Science
and Technology (NTNU)
Trondheim, Norway

Torgeir Moan

Centre for Ship and Ocean
Structures (CeSOS)
Centre for Autonomous Marine
Operations and Systems
(AMOS)
Norwegian University of Science
and Technology (NTNU)
Trondheim, Norway

ABSTRACT

The STC (Spar Torus Combination) concept combines a Spar floating wind turbine and a torus-shaped heaving-body wave energy converter (WEC). Numerical simulation has shown positive synergy between the WEC and the Spar floating wind turbine in operational conditions. However, in extreme wind and wave conditions, it is challenging to maintain structural integrity, especially for the WEC. To ensure survivability of this concept in extreme conditions, three survival modes have been proposed.

To investigate the performance of the STC in extreme conditions, model tests with a scale factor of 1:50 were carried out in the towing tank of MARINTEK, Norway. Two survival modes were tested. In both modes, the Torus WEC was fixed to the Spar. In the first mode, the Torus WEC is at the mean water surface, while in the second mode, the Torus WEC is fully submerged to a specified position. In the tests, 6 D.O.F rigid body motions, mooring line tensions, forces in 3 directions (X, Y and Z) between the Spar and Torus were measured, wind velocity and wind force were also measured by a sensor in front of the model and a load cell installed on the wind disc.

In this paper, the model test set-up for the two survival modes are described, and then decay tests, regular wave tests and the statistical tests for wind only, irregular wave only and irregular wave plus wind are presented, compared and analyzed. In the mean water level survival mode, the Torus had a small draft and large water plane area, so slamming and green water were observed as expected. In addition, Mathieu instability phenomena were observed during the regular wave test. In some large wave conditions in the fully submerged mode, no severe wave load occurred. All the results are presented in model scale unless specified, for direct comparison with numerical simulations later.

Key words: Spar Torus Combination, Wind Turbine, Wave Energy Converter, Model Test, Survival Mode, Slamming, Mathieu Instability.

INTRODUCTION

Offshore wind farms are becoming more and more attractive due to abundant and steady wind resources. In shallow water, the fixed wind turbine can be cost effectively installed and easily maintained. In deep water, floating wind turbines become necessary. Wave energy also represents a significant resource with great potential. The World Energy Council has conservatively estimated the market potential for wave energy to be in excess of 2,000TWh/year [1]. In this paper, a combined concept of offshore wind and wave energy, named STC (Spar and Torus Combination), is presented, and model tests of this concept with an emphasis on survival conditions are described.

The STC (Spar Torus Combination) concept as shown in Figure 1 combines a spar floating wind turbine and torus-shaped heaving body wave energy converter (WEC) [2]. The floating wind turbine is the 5 MW NREL reference machine [3]. The wave energy converter is inspired by the Wavebob concept [4], which has been developed from 1999 to 2013. In the STC concept, the torus can move along the cylinder of the spar to absorb wave energy. A mechanical system is provided to limit the relative horizontal motion between the two bodies, and an end stop system can limit the excessive relative heave motion in extreme conditions. The spar floater provides a support structure for the WEC, while both can share the same cable and mooring systems. Past numerical simulation made [5] show positive synergy between the two bodies in operational

sea states. However in extreme conditions, this concept, especially the WEC, is subjected to severe loads [6]. Hence survival modes are needed for the STC concept to ensure structural integrity. In [6], three survival modes were considered for the STC and numerical simulations were carried out for two modes to estimate the motions and forces on the structure. The three survival modes are illustrated in Figure 2 and are described as follows:

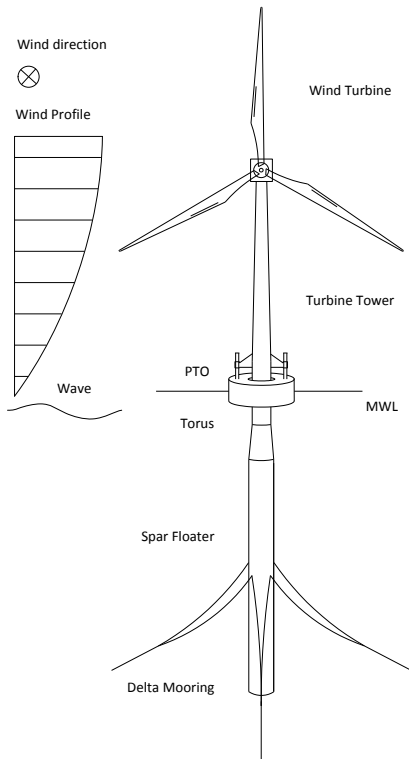


Figure 1. STC concept

Mode I: the WEC PTO system is released, the wind turbine is parked, the torus moves freely along the Spar. The motion is limited only by the end stop system. It is referred to as the released mode hereafter.

Mode II: the WEC PTO system is released, the wind turbine is parked, and the torus is locked mechanically to the spar at the mean water level (MWL). In this mode, the two bodies are locked and move together. It is referred to as MWL mode hereafter.

Mode III: the WEC PTO system is released, the wind turbine is parked, and the torus is locked mechanically to the spar. By adding ballast to the Torus or the bottom of the spar, the two bodies are submerged to a specified position. In this mode, the torus is totally submerged (SUB) in the water. This mode is referred to as SUB mode hereafter.

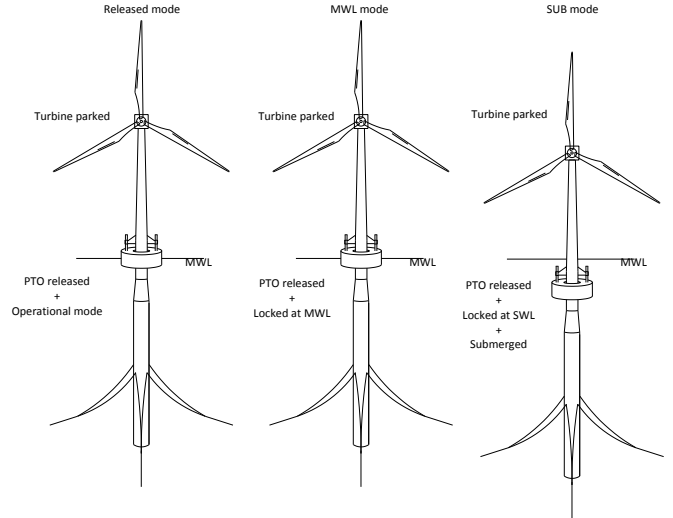


Figure 2. Configurations for the 3 survival modes

Numerical simulations were carried out for the first two modes, and showed that the maximum horizontal contact force and vertical locking force for MWL mode and the maximum horizontal contact force and vertical end stop force for released mode increase significantly for extreme conditions compared to operational conditions. In released mode, the contact and end stop force are significantly larger than that for the MWL mode [6]. The released mode is not a possible survival mode, but considered just as a comparison. In the model test, the focus was put on the MWL and SUB modes to investigate the strategy for survivability.

MODEL TEST SET-UP

The model tests with focus on extreme conditions were carried out in the towing tank of MARINTEK, Norway. The model was down scaled by Froude scaling with a ratio of 1:50. The scaling factors for different variables by Froude scaling are listed in Table 1.

Table 1. Froude scaling of the variables

Variables	Symbol	Scale factor	Value
Linear Dimensions	D	λ	1:50
Fluid or structure velocity	u	$\lambda^{1/2}$	1:7.07
Fluid or structure acceleration	a	1	1:1
Time or period	t	$\lambda^{1/2}$	1:7.07
Structure mass	m	λ^3	1:1.25 $\times 10^3$
Structure displacement volume	V	λ^3	1:1.25 $\times 10^5$
Force	F	λ^3	1:1.25 $\times 10^5$
Moment	M	λ^4	1:6.25 $\times 10^6$

The STC model is shown in Figure 3. The tower and main part of the floater are made of PVC, the cylinder in the middle part which is also the upper part of the spar floater is made of aluminum alloy. This choice was made to provide high stiffness for installing the load cells between the two bodies. The torus is made of two materials, with a core material of Dyvinnell and aluminum alloy plates on the top and bottom. The catenary delta mooring system is modeled here as 3 rigid bars connected by 3 linear springs. The wind force on the wind turbine is

simulated by two wind discs of different diameters, with a small disc to model the thrust force in extreme wind condition, and a large disc to model the thrust force in operational conditions. The wind velocity is down scaled by Froude scaling, and based on the designed thrust force and wind velocity, the disc diameter can be decided assuming a drag coefficient of 1.2. In Figure 3, the mooring system, tower, floater and wind discs are shown; and the coordinate system is also indicated. The coordinate of the model test is set as follows: z direction is positive downward, x direction is positive in the upwind direction. The origin is assumed to be the intersection point of the still water surface and the central line of the cylinder. The wind and waves aligned in the tests.

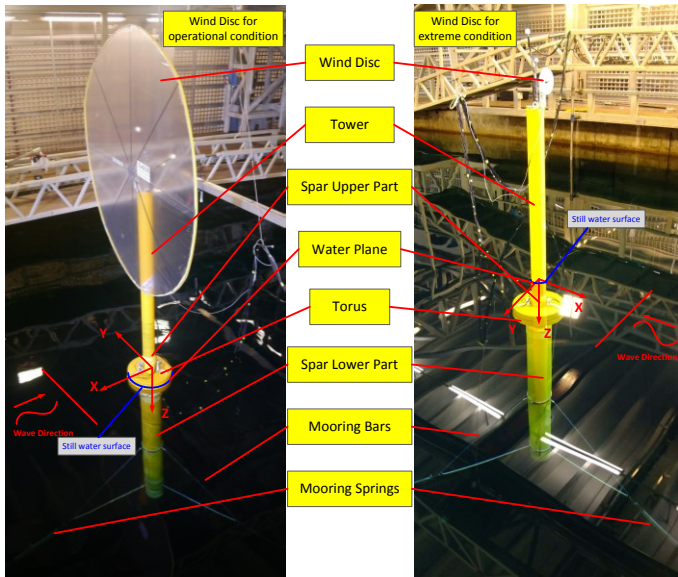


Figure 3. Model and coordinate system

The most critical part is the connection between the two bodies, which is shown in Figure 4. The spar and the torus are rigidly connected by 18 load cells that are provided to measure the forces in 3 directions at 6 positions, of which 3 are located on the top of the torus 120 degrees apart, and 3 others are located on the bottom. At each position, 3 load cells are installed orthogonally to measure forces in 3 local directions. Then the total force can be calculated from these load cell measurements.

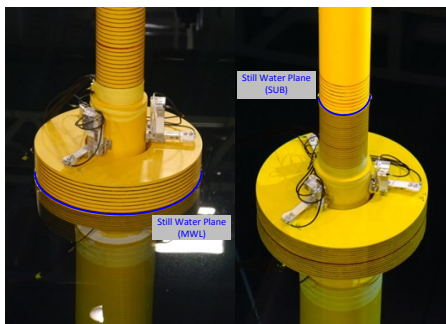


Figure 4. The two survival modes considered

As mentioned above, MWL and SUB survival modes are the focus of the model tests, so the performance of the model during extreme conditions for these two survival modes is tested and investigated. In the MWL mode, the torus is on its mean water surface, while in the SUB mode, the torus is totally submerged at a specified position by additional ballast in the bottom of the Spar. The two modes are shown in Figure 4. The dimension and weight information for the model is shown in Table 2, Table 3 and Table 4.

Table 2. Model dimensions

Spar & Tower		Model Scale [m]	Full Scale [m]
Spar lower part	Diameter	0.2	10
	Length	2.16	108
Spar upper part	Diameter	0.129	6.45
	Length	0.48	24
Tower	Diameter	0.11	5.5
	Length	1.54	77
Torus			
	Height	0.16	8
	Outer diameter	0.4	20
	Inner diameter	0.16	8

Table 3. Draft of the model in different survival modes

	MWL mode [m]	SUB mode [m]
Spar & Tower	2.44	2.96
Torus	0.08	Totally submerged

Table 4. Weight data for the single-body model and the two-body model

STC		MWL mode	SUB mode
Total weight (including Ballast) [kg]		80.29	94.72
Ballast [kg]		34.21	48.64
C.O.G from WL [m]		1.35	2.00
C.O.G from Geometric centre of Torus [m]		1.35	1.48
Radius of gyration with respect to water line [m]	Rxx	1.77	2.28
	Ryy	1.77	2.28
	Rzz	0.09	0.09
Spar & Tower			
Total weight (including Ballast) [kg]		71.13	85.56
Ballast [kg]		34.21	48.64
C.O.G from WL [m]		1.53	2.16
Radius of gyration with respect to water line [m]	Rxx	1.89	2.40
	Ryy	1.89	2.40
	Rzz	0.08	0.08
Torus			
Total weight [kg]		9.16	9.16
Ballast [kg]		-	-
C.O.G from WL [m]		0.00	0.52
Radius of gyration with respect to water line [m]	Rxx	0.14	0.53
	Ryy	0.14	0.53
	Rzz	0.14	0.14

TEST MATRIX

The test procedure is described in the following:

Firstly, structural tests were carried out at several points on the spar and the torus before and after putting the model in the water to identify the main dry and wet structural eigen-frequencies.

Secondly, decay tests were performed for the 6 degrees of freedom (D.O.F). From the rigid body motion, the natural period and damping level can be determined.

Thirdly, regular wave tests were performed to determine the RAO of the model. The regular wave periods varied from 0.99s to 3.253s in model scale, and two sets of regular wave heights were tested, i.e. H=0.04m and H=0.18m, for the purpose of assessing the nonlinearity of the response.

Then, tests in irregular waves only were considered. Three sea states were selected, with one operational sea state (Hs=0.055m, Tp=1.57s) and two extreme sea states (Hs=0.27m, Tp=2.121s and Hs=0.306m, Tp=2.192s). The waves follow the Jonswap Spectrum, and for each sea state, several tests were performed with different random seeds.

Finally, wind only tests and irregular wave plus wind tests were performed. For the tests with wind, two discs were used to have representative mean thrusts in operational and survival conditions. In operational wind condition, the large wind disc should be used and in extreme wind the small disc should be used. The wind velocities are also downscaled by the Froude scaling.

It is noted that all the test procedures were generally the same for the MWL and SUB modes.

MODEL DECAY TEST

In the first stage of model testing, decay tests were carried out to identify the natural period and damping of the 6 degree D.O.F. For low damping ratio, typically $\zeta < 0.2$, the logarithmic decrement Λ and the damping ratio ξ have the relationship as follows:

$$\Lambda = \ln \left(\frac{x_i}{x_{i+n}} \right) / n \quad \Lambda = \xi \omega_0 T_d = 2\pi \frac{\xi}{\sqrt{1-\xi^2}} \approx 2\pi\xi \quad (1)$$

in which, x_i is the i-th cycle amplitude, T_d is damped oscillation period, which is measured from decay time series. The damping listed here is the equivalent damping calculated from oscillations without transient effect, i.e. calculated from the third or more oscillations from the beginning of the decay.

Several decay tests were performed for each D.O.F. The decay test data is referred to the Center of Gravity (C.O.G) of the model, which is 2 m below water line in SUB mode, and 1.35 m below water line in MWL mode. The surge and heave decay time series and the corresponding peaks for SUB mode is shown in Figure 5. The decay time series for MWL mode is shown in Figure 6. The time axis shows the real time of recording during the test.

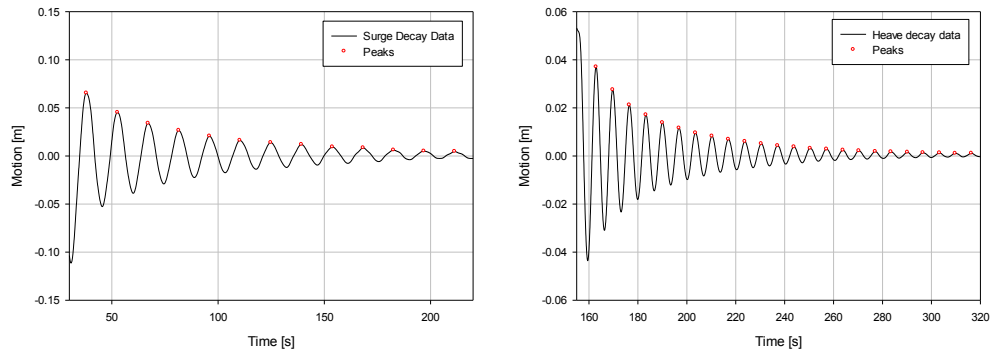


Figure 5. Decay time series for Surge and Heave of SUB mode

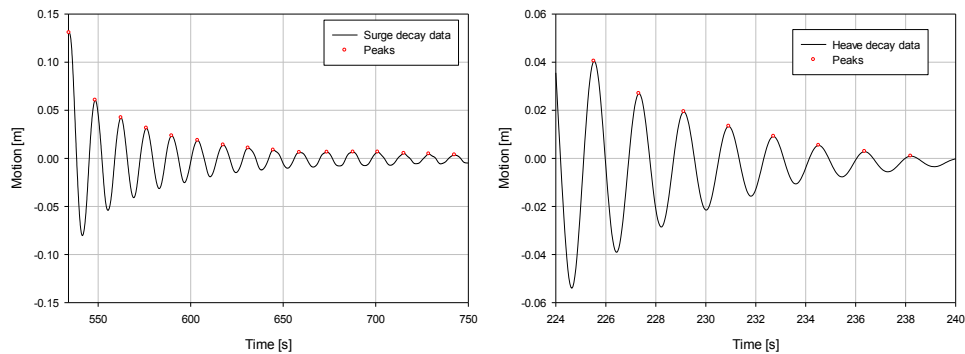


Figure 6. Decay time series for Surge and Heave of MWL mode

The identified model parameters from the decay tests are listed in Table 5. For the yaw decay, supercritical damping was observed and the motion took only one cycle to die out. This might be due to the 3 long rigid mooring bars. When performing the yaw decay, the mooring bars had the spring forces in tangential directions, and there was deformation of the bars, then structural damping played a significant role. Because the bars are quite long, the drag of bars was also a contribution to the damping. In the prototype model, delta mooring configuration provides large yaw stiffness and leads to really small yaw motion, which was corrected modelled by the mooring bars in the tests. For the pitch and roll decay test, there is always coupling with surge, so it is hard to identify the damping ratio in pitch and roll. It can be seen that by changing mode from MWL to SUB, the heave natural period increases from 1.8s to 6.7s, the pitch natural period also increases due to different moment of inertia of the two modes, while the surge natural periods are generally the same.

Table 5. Decay test results

D.O.F	SUB			MWL		
	T_m [s]	T_f [s]	ξ	T_m [s]	T_f [s]	ξ
SURGE	14.42	102	0.034	13.86	98	0.04
SWAY	13.09	93	0.046	13.17	93	0.04
HEAVE	6.67	47	0.024	1.81	13	0.07
ROLL	3.62	26	0.027	5.09	36	-
PITCH	3.63	26	0.023	5.18	37	-

Comments: T_m is period in model scale, T_f is period in full scale, ξ is the damping ratio from the decay test.

REGULAR WAVE TEST

The regular wave tests were carried out to determine the response amplitude operator (RAO) as well as possible nonlinear effects for large waves. It shows the response under sinusoidal waves for different wave periods and wave heights. For each survival mode, several wave periods and two wave heights were chosen for testing. The small wave height is 0.04 m and the large one is 0.18 m. The RAO is only defined when the response is assumed to be linear, and the output frequency is the same as input frequency. When there is a strong nonlinear response, e.g. water exit and water entry, there might be different frequency in response, so the amplitude ratio between response and wave rather than RAO is more precise. The amplitude ratio is calculated by dividing the steady state response height by the simultaneous wave height. For each test case, the calculation was based on four sinusoidal cycles in the steady state response, and then there are four values showing the scatter of the results. It should be noted that the response values of the motions are all referred still water level (SWL) position of the center of the cylinder.

The regular wave test matrix and the occurrence of nonlinear phenomena are shown in Table 6. It is noted that in the test, strongly nonlinear phenomena were observed during the regular wave tests. For a WEC, the natural period should be located in the frequent wave period region. In the MWL mode, the heave natural period is about 1.8s (12.7s in full scale),

which is excited during the regular wave test. Moreover, due to the small draft of the torus, water exit and water entry phenomena are expected to occur. ‘Slamming’ [7] is often referred to as impulse loads with high pressure peaks occur during impact between a body and water. In addition, global elastic transient resonant oscillation which is referred to as ‘whipping’ could also be excited in connection with slamming. When the model has large heave motion, the torus is totally out of water, and when the torus is entering the water, there will be impact between its bottom and the water. This is very dangerous for the WEC and the interface between the Torus and the Spar, because the impact will induce large loads depending on the local structure-fluid relative velocity and the local geometry in the impact region (dead-rise angle). Moreover, slamming events are not periodic and not repeatable, even in regular wave tests.

Table 6. Regular wave test matrix and the occurrence of nonlinear phenomenon

Test mode	MWL		SUB	
H [m]	0.04	0.18	0.04	0.18
T [s] M/F				
0.990/7		-		-
1.273/9		Slamming and green water		
1.556/11				
1.697/12	Slamming		-	-
1.839/13				
1.980/14			-	-
2.121/15				
2.405/17		Mathieu instability		
2.687/19				
2.970/21				
3.253/23				VIM
3.536/25	-	-	-	

Comment: - means no wave test for this period; M: model scale; F: full scale

In Table 6, it can be seen that for the MWL mode, during regular wave test with small wave height (H=0.04 m), water exit was observed only in the heave resonance period region, i.e. T=1.697s and T=1.839s. The occurrence of slamming increases the forces between the bodies significantly. For large wave height (H=0.18 m) in MWL mode, due to the small torus draft, slamming and green water can be observed with most of the wave periods. For T=2.405s, which is a quite long wave, Mathieu-type instability was observed around 100s after generating waves. In this case, the pitch motion period is evolving gradually from the wave period until twice the wave period, while the pitch amplitude is also growing until a steady state. When analyzing the time series, the response might not have a single harmonic signal when there are strongly nonlinear effects, e.g. the slamming and green water will induce structural vibration and the impact force might be even larger than the wave induced force; the Mathieu-type instability will take place at a frequency other than the wave frequency. In these cases, maximum and minimum values for one cycle in the steady state regime are used for the calculation of the RAO. Slamming and Mathieu instability are further discussed later in this paper.

For very long waves with wave periods T=3.253s and T=3.536s, the transverse motions (sway and roll), as well as

yaw motion were observed to increase gradually for the SUB mode. It might due to the vortex-induced motion (VIM).

Figure 7 - Figure 9 show the surge, pitch and heave-wave amplitude ratio for different wave heights in the two survival modes. Figure 10 - Figure 11 show the amplitude ratio for the force between spar and torus in the X- and Z-directions (FX and FZ) on spar for the large and small wave height in the two modes. In these plots, the slamming and instability cases as well as the heave and pitch natural periods are also included.

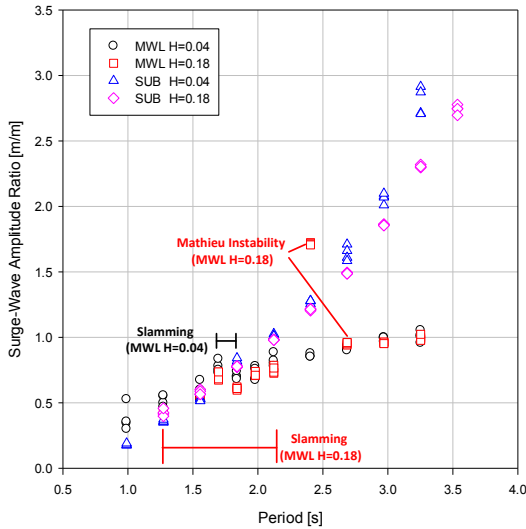


Figure 7. Surge-wave amplitude ratio in the two survival modes

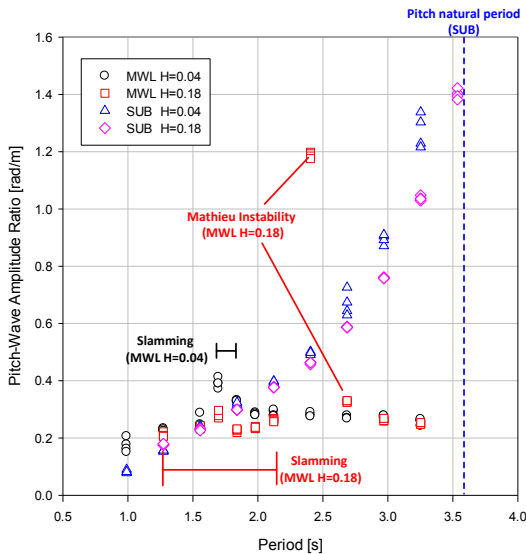


Figure 8. Pitch-wave amplitude ratio in the two survival modes

MWL mode

In the MWL mode, it can be seen from pitch and surge-wave amplitude ratio that they have generally the same trend, which means that the surge is mainly induced by pitch. It is

really hard to get the pure surge and center of pitch during the regular wave tests due to the long Spar geometry. In addition, the surge resonance period is around 100s in full scale, which is far from the wave period. For pure surge motion, focus should be on the slowly varying motion, which will not be discussed in detail in this paper. For H=0.04m of MWL mode, there is a small jump for the case of T=1.839s and T=1.697s in surge and pitch amplitude ratio, this is due to the water exit of torus, and in heave motion, the jump is quite obvious because these two periods are in the heave resonance region.

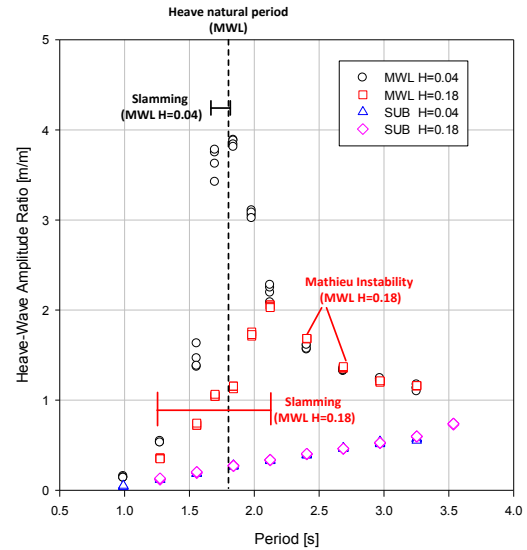


Figure 9. Heave-wave amplitude ratio in the two survival modes

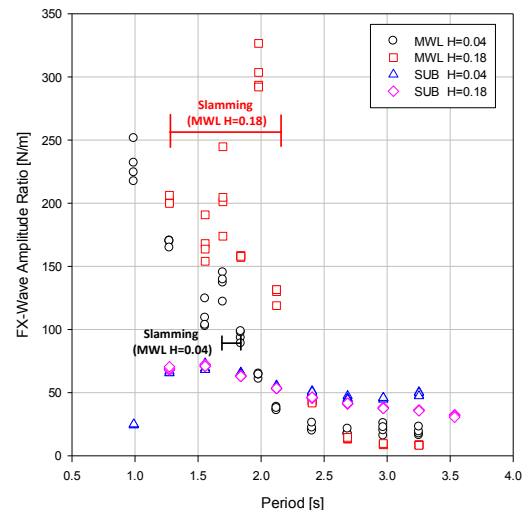


Figure 10. FX-wave amplitude ratio in the two survival modes

For H=0.18m, the surge and pitch-wave amplitude ratio generally follow the same trend as for H=0.04m except for T=2.405s, when strong Mathieu instability occurs. For the case T=2.405s, in steady state, the pitch motion is increased

significantly and the amplitude ratio is much larger. At the same time, the pitch period is changing from the wave period to twice the wave period, which is shown in Figure 13. For $T=2.687s$, the instability was not fully developed, which means that the main period for pitch is still the wave period and the motion has not increased significantly, which is shown in Figure 14.

For heave motion, the amplitude ratio is not affected much by the Mathieu instability, but in the slamming region, it is totally different from the amplitude ratio for small wave height.

It can also be seen from Figure 10 that in the slamming region, FX has much larger values than that in the non-slamming region, and there is a jump at $T=2.121s$ which divides the slamming and non-slamming regions. When the Torus is entering the water, it is not exactly upright as the still water floating condition, so there is a pitch angle, which will induce a force in the X direction. In Figure 11, the FZ-wave amplitude ratio follows the same trend as that in heave motion. In the force channels, when there is slamming, the model will vibrate, and the force signals have quite high frequencies other than the wave frequency. In some cases, the slamming forces are even higher than forces induced by waves. The amplitude ratios use only the maximum and minimum values no matter whether the maximum or minimum value is induced by the wave or not.

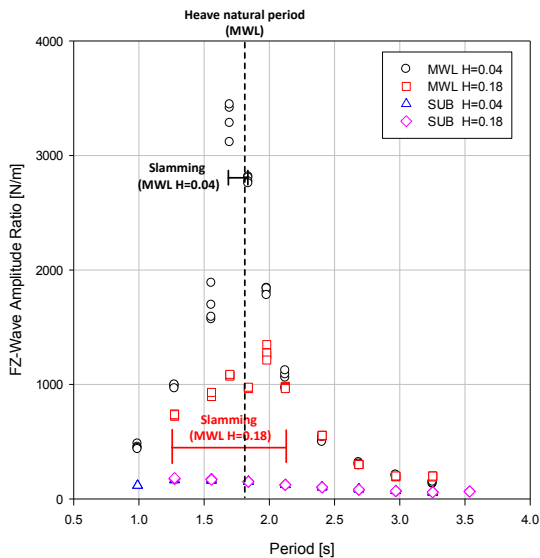


Figure 11. FZ-wave amplitude ratio in two survival modes

SUB mode

For the SUB mode, no slamming and Mathieu instability were observed, so the motion response can be assumed to be linear or weakly nonlinear. It can be seen quite obviously through surge and pitch RAOs that the damping plays a more important role for the large wave height and near the resonance period. For heave motion, the difference of RAO between large and small wave heights is not so obvious.

Comparison between the two modes

It can be seen that by changing the mode from MWL to SUB, the heave and pitch resonance periods change. The heave natural period is out of the wave period range for SUB mode, while the pitch natural period is closer to the wave period range for SUB mode than MWL mode. From the force channels, it is very obvious that the forces for SUB model are reduced significantly than that in MWL mode.

SLAMMING

From Table 6, it can be seen that slamming occurs for a large region in the regular wave test matrix in MWL mode. For the case $H=0.18m$, $T=1.697s$, the time series of FX and FZ from 73s-75s as well as the motion and velocity of the model are plotted in Figure 12 with snapshots from the videos in the test. It is nearly one sinusoidal cycle for the wave.

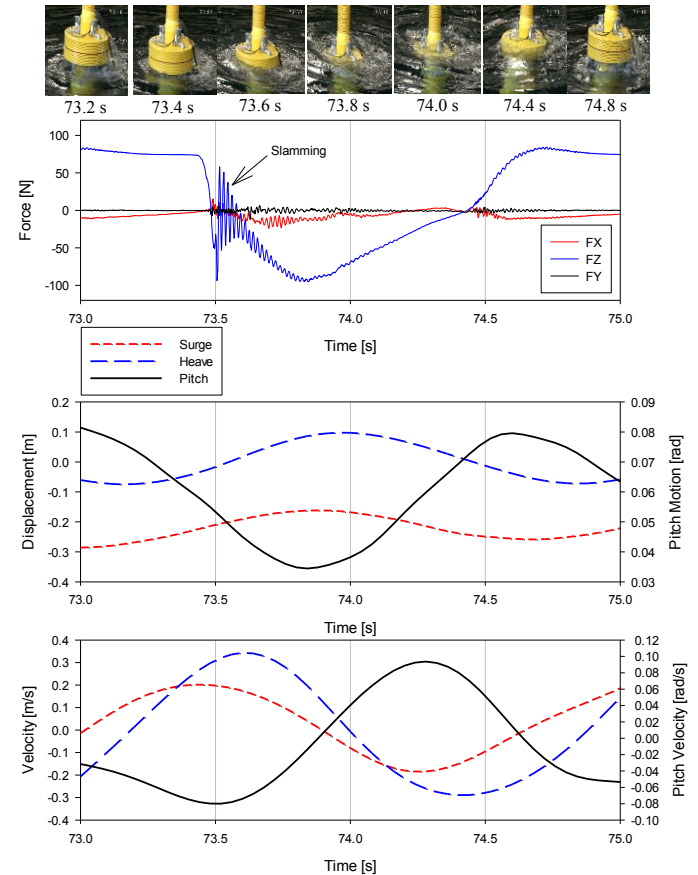


Figure 12. Example of slamming and green water time series

It can be seen that due to water exit and water entry, the forces between the two bodies are strongly increased. This regular wave cycle can be divided into several phases with different phenomena.

For phase I, 73.0-73.4, the torus is out of water, but there is still some water on deck. In this phase, FZ is dominated by the

inertia force, in which case is positive (pointing downward) and nearly constant.

For phase II, 73.4-73.8, the Torus starts entering the water; at the beginning of this phase, there is an impact force, then the vertical force increases significantly until the minimum occurs (pointing upwards) with local structural vibration due to slamming. The impact force has a frequency of around 65Hz, which is close to the eigen-frequency from the hammer tests. The heave velocity reaches a maximum when slamming just occurs.

For phase III, 73.8-74, the structure continues entering the water until the heave motion reaches maximum, and green water occur, the torus submerges into the water. In this phase, the structural vibration vanishes.

For phase IV, 74-74.4, the torus starts moving upwards until the top exits the water. There is still green water on deck, although the water amount on deck decreases gradually. FZ changes linearly in this phase.

Then it goes to phase I again, 74.4-74.7. In the beginning, air gap between water and the torus bottom emerges and increases, and there is a suction force pointing downward. Now, the torus is totally out of the water, and there is no wave force on the Torus.

Further investigation is needed for slamming prediction and analysis, a fully nonlinear method is necessary for accurate analysis of the slamming phenomenon.

MATHIEU-TYPE INSTABILITY

A nonlinear phenomenon known as Mathieu-type instability was observed in the case of $H=0.18$ m, $T=2.405$ s (regular wave test). In this case, the pitch motion was unstable and started to increase from around 70s until a steady state was achieved, when the pitch motion period (around 4.8s) is twice the wave period (2.4s), while the pitch natural period is 5.1s from the decay test. Figure 8 shows that the Mathieu instability cases have the pitch values much larger than in other cases. In the pitch steady state, the heave motion also followed two frequencies with an envelope, as shown in Figure 13. Even if the instability evolves until a steady state, the pitch motion was not pure sinusoidal, it had also small wave frequency. This might due to the fact that the wave period is not exactly $\frac{1}{2}$ of the pitch natural period.

In the regular wave case $H=0.18$ m, $T=2.687$ s, there was also a sign of instability, as the pitch follows two periods (wave period and double wave period), but the wave period motion

has more energy as shown in Figure 14. It can be taken as a Mathieu instability which is not fully developed.

There are different kinds of Mathieu instability [8][9]. When the Spar has an abrupt change in the water plane area, there will be a change in the heave restoring force, which is time dependent. Then the undamped equation of motion can be expressed as:

$$[M + A_{33}]\ddot{\eta}_3 + [k_3 + \Delta k_3 f(t)]\eta_3 = 0 \quad (2)$$

in which, M is the structural mass; A_{33} is the heave added mass; η_3 is the heave motion; $\ddot{\eta}_3$ is the heave acceleration, k_3 is the heave restoring coefficient and $\Delta k_3 f(t)$ is the time dependent heave restoring. Equation 2 has the same form as Mathieu's equation. The heave motion will follow the wave frequency, so is the heave restoring due to the abrupt change of the water plane area.

Another kind of Mathieu instability is the heave/pitch coupled instability. This is due to the influence of heave on the pitch restoring term. If the damping term is neglected, the uncoupled pitch equation of motion can be expressed as:

$$[I_{55} + A_{55}]\ddot{\eta}_5 + \rho g V \overline{GM} \eta_5 = 0 \quad (3)$$

where I_{55} is the pitch moment of inertia, A_{55} is the pitch added moment, ρ is the water density, g is the gravity acceleration, V is the buoyancy volume, $\ddot{\eta}_5$ is the pitch acceleration and η_5 is the pitch motion.

$$\overline{GM} = \overline{GM}_m - \frac{1}{2}(\eta_3(t) - \zeta(x_c, y_c, t)) \quad (4)$$

$$V = V_m - A_w(\eta_3(t) - \zeta(x_c, y_c, t)) \quad (5)$$

where \overline{GM}_m is the pitch metacentric height associated with the restoring at still water, V_m is the still water displaced volume, A_w is the water plane area, η_3 is the heave motion and $\zeta(x_c, y_c, t)$ is the wave elevation at the center of flotation, x_c and y_c are center of flotation coordinates. If the heave motion is assumed to be $\eta_3(t) = \eta_{3m} \cos(\omega t)$, where ω is the heave motion frequency, η_{3m} is the heave amplitude and the wave elevation effect is ignored, then equation 3 can be expressed as:

$$[I_{55} + A_{55}]\ddot{\eta}_5 + \rho g V (\overline{GM}_m - \frac{1}{2} \eta_{3m} \cos(\omega t)) \eta_5 = 0 \quad (6)$$

Equation 6 is the classical Mathieu equation. Considering the damping, stability diagram can be generated [9], which shows the unstable region. The unstable region is reduced when damping is added to the system. Based on the stability diagram, if ω_5 is the pitch natural period, when ω_5/ω is around 0.5, 1, 1.5, 2 and so on, the instability might happen. In the case of this model test, Mathieu instability occurred when ω_5/ω is close to 0.5. The Mathieu instability belongs to the heave-pitch coupled type. Further investigation is needed to predict the Mathieu instability in simulations.

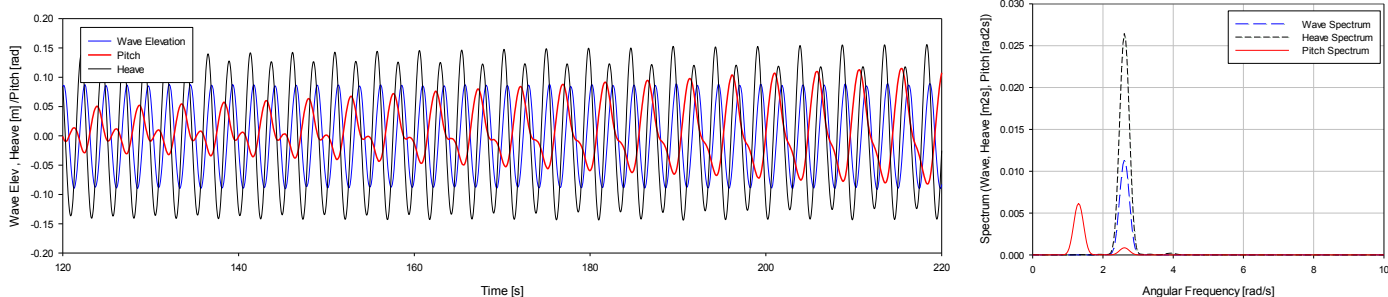


Figure 13. Motion in a regular wave H=0.18m, T=2.405s with Mathieu instability

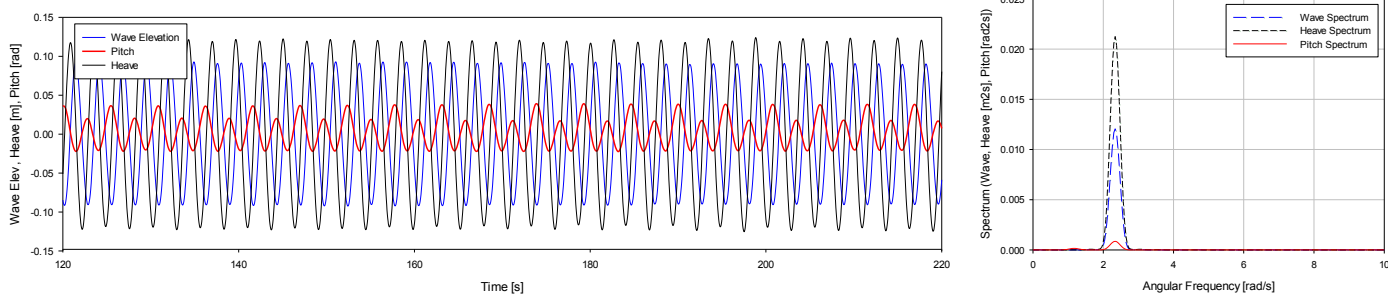


Figure 14. Motion in a regular wave H=0.18m, T=2.687s with Mathieu instability not fully developed

TESTS WITH IRREGULAR WAVES AND WIND

The response of the STC in irregular waves with different sea states was tested. Three sea states were selected in this model test, one operational sea state and two extreme sea states, of which one is selected by maximum mean wind speed U_w at 10m height and the other one is selected by maximum significant wave height H_s [10]. During the test, however, it was found to be hard to generate the desired wind speed accurately, so for the two extreme sea states, the same wind speed was used. The designed site for the model is 30 km from the west coast of Norway which is Site 14 in [10]. The selected test matrix for irregular waves and wind test are shown in Table 7. In this table, model scale and prototype values are presented.

As mentioned above, two discs with different diameters were used. The purpose was to model the correct wind thrust force. The wind velocity was downscaled by Froude scaling, then by the thrust force formulation: $T = \frac{\rho A}{2} C_d V^2$, with $C_d=1.2$, two disc diameters can be calculated corresponding to the two wind speeds. In the test, the wind was generated by an array of fans, and in the wind time series, a large turbulence was observed. In addition, it was hard to control the wind speed accurately as desired, so the actual wind speed was a little different. For extreme wind, about $U_w=5.5$ m/s was achieved, with an STD of 0.5 m/s and for operational condition, about $U_w=1.3$ m/s was achieved with an STD of 1.6 m/s. U_w measured is the absolute wind velocity, not the relative velocity between wind and platform motion. STD is the standard

deviation of the wind time series for the steady state regime of the model motion (300s-900s).

Table 7. Irregular wave and wind test matrix

	Sea States	H_s [m]	T_p [s]	U_w [m/s]
Wind only	Operational	-	-	1.61/11.4
	Extreme	-	-	4.70/33.3
Irregular wave only	Operational	0.055/2.75	1.570/11.0	-
	Extreme 1	0.270/13.5	2.121/15.0	-
	Extreme 2	0.306/15.3	2.192/15.5	-
Irregular wave +wind	Operational	0.055/2.75	1.570/11.0	1.61/11.4
	Extreme 1	0.270/13.5	2.121/15.0	4.70/33.3
	Extreme 2	0.306/15.3	2.192/15.5	4.70/33.3

For the irregular wave tests with and without wind, 900s time series were recorded, with the last 600s used for the statistical analysis. For one sea state, several tests were carried out with different seed numbers. The generated waves followed the 3-parameter Jonswap spectrum with H_s , T_p and $\gamma=3$.

It was observed during the irregular wave test that slamming occurred frequently during extreme sea states in the MWL mode, but in the SUB mode, slamming only occurred in the cases where the wave was so steep that it hit the tower of the model and caused slamming force. In operational sea states, there was also some green water or occasional slamming for the MWL mode.

The response in the SUB mode is expected to be much smaller than that in the MWL mode. The surge motion and force FZ in SUB and MWL modes for several test cases are

listed in Figure 15 and Figure 16. The surge motion is referred to the still water line position. The statistical values include mean, STD, maximum and minimum values.

Figure 15 shows that the mean surge is mainly induced by wind, while the STD is mainly dominated by wave, which is also expected from the simulation in [6]. From Figure 16, it can be observed that even without wind, there is still a large mean surge, this might partly due to the large radiation of the torus, and partly due to the water exit and entry, both of which will induce mean drift. The wind also gives a large mean surge as in

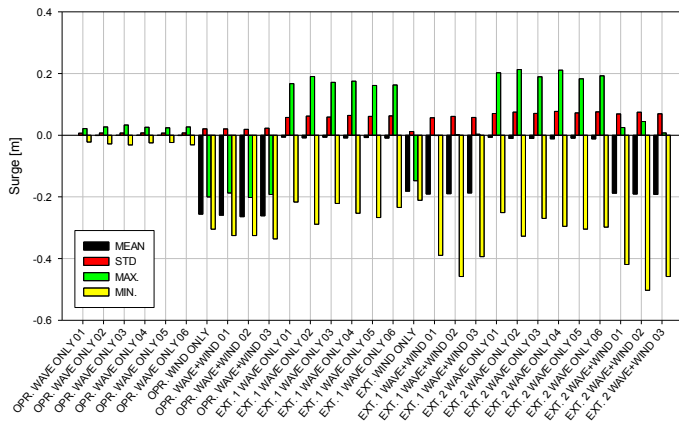


Figure 15. Statistical values of surge motion and force FZ in different test cases for the SUB mode

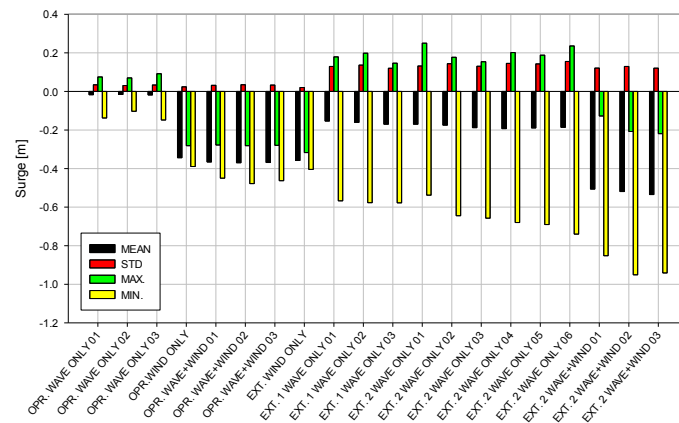
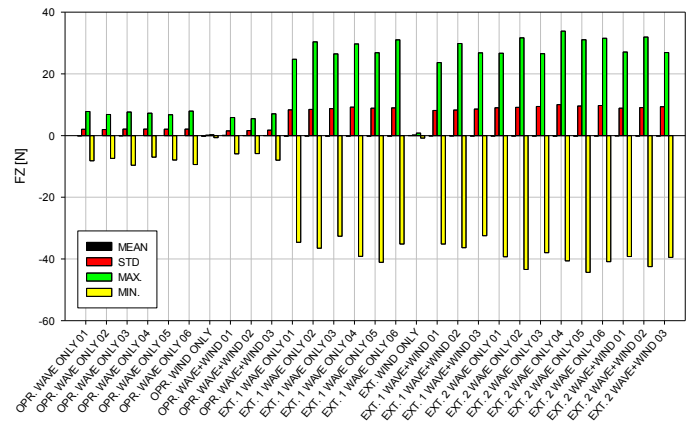
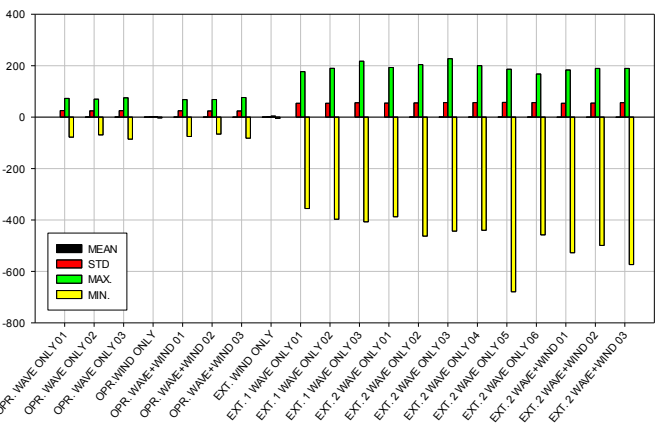


Figure 16. Statistical values of surge motion and force FZ in different test cases for the MWL mode

It is expected that for the SUB mode, the motion and force will decrease significantly. For instance, it can be observed in Figure 15 and Figure 16 that the FZ force is much smaller (about 1/10-1/7) in the SUB mode than that in the MWL mode. Similar results hold for the heave motion, which are not shown in this paper. The surge and pitch motions are also reduced, but not as significantly as the heave.

SUB mode. With the operational case in MWL mode, the main surge is dominated by the wind.

In extreme conditions, the maximum and minimum forces are all due to water exit and water entry. It can be seen from Figure 16 that the extreme wind increased the absolute value of the FZ in minus direction (upward) in MWL mode, it means the wind made the slamming stronger. This might due to the wind increasing the motion, and causing larger relative velocity between the model and water. At the same time, the wind might also change the dead-rise angle of the model when entering the water.



CONCLUSION REMARKS

The model tests show that the SUB mode is a possible solution for the survivability of the STC concept in extreme conditions. By submerging the model, the motion and the forces between spar and torus are decreased; hence it will be less challenging for designing the interface between the two bodies both from fatigue and ultimate strength limit state points of view.

The special nonlinear phenomena observed during the tests revealed interesting issues regarding the STC concept. More investigation on the water exit and water entry, and the Mathieu instability cases need to be carried out through simulation especially for the MWL mode.

Time domain simulations including nonlinear features are needed for the analysis of the combined concept. The simulation and analyses should be validated by the test results in the near future.

ACKNOWLEDGMENTS

The authors gratefully acknowledge the financial support from the European Commission through the 7th Framework Programme (MARINA Platform –Marine Renewable Integrated Application Platform, Grant Agreement 241402), Center for Ships and Ocean Structures (CeSOS), NTNU and China Scholarship Council (CSC).

REFERENCES

- [1] <http://www.pelamiswave.com/global-resource>, accessed on 10th, Dec, 2013.
- [2] Muliawan, M.J., Karimirad, M., Moan, T., Gao, Z. STC (Spar-Torus Combination): a combined spar-type floating wind turbine and large point absorber floating wave energy converter - promising and challenging. Proceedings of 31st International Conference on Ocean, Offshore and Arctic Engineering OMAE2012-84272. Rio de Janeiro, Brazil.
- [3] J. Jonkman, S. Butterfield, W. Musial, and G. Scott. Definition of a 5-MW Reference Wind Turbine for Offshore System Development. Technical Report NREL/TP-500-38060. February 2009.
- [4] <http://en.wikipedia.org/wiki/Wavebob>, be accessed in 2nd, January, 2014.
- [5] Muliawan, M.J., Karimirad, M and Moan, T. Dynamic Response and Power Performance of a Combined Spar-type floating Wind Turbine and Coaxial Floating Wave Energy Converter. *Renewable Energy* 50 (2013), 47-57.
- [6] Muliawan, M.J., Karimirad, M., Gao, Z., Moan, T. Extreme responses of a combined spar-type floating wind turbine and floating wave energy converter (STC) system with survival modes. *Ocean Engineering* 65 (2013), 71–82.
- [7] O.M.Faltinsen. *Sea Loads on Ships and Offshore Structures*. Cambridge University Press, 1990.
- [8] H.A. Haslum, O.M. Faltinsen. Alternative Shape of Spar Platforms for Use in Hostile Areas. OTC 10953, 1999.
- [9] B.J. Koo, M.H. Kim, R.E. Randall. Mathieu instability of a spar platform with mooring and risers. *Ocean Engineering* 31 (2004), 2175-2208.
- [10] Li, L., Gao, Z. and Moan, T. (2013) Joint Environmental Data at Five European Offshore Sites for Design of Combined Wind and Wave Energy Devices. Proceedings of the 32nd International Conference on Ocean, Offshore and Arctic Engineering, OMAE2013-10156, Nantes, France.